# Towards Modeling the Traffic Data on Road Networks

Ugur Demiryurek, Bei Pan, Farnoush Banaei-Kashani and Cyrus Shahabi
Department of Computer Science
University of Southern California
Los Angeles, CA 90089
{demiryur,beipan,banaeika,shahabi}@usc.edu

## ABSTRACT

A spatiotemporal network is a spatial network (e.g., road network) along with the corresponding time-dependent weight (e.g., travel time) for each edge of the network. The design and analysis of policies and plans on spatiotemporal networks (e.g., path planning for location-based services) require realistic models that accurately represent the temporal behavior of such networks. In this paper, for the first time we propose a traffic modeling framework for road networks that enables 1) generating an accurate temporal model from archived temporal data collected from a spatiotemporal network (so as to be able to publish the temporal model of the spatiotemporal network without having to release the real data), and 2) augmenting any given spatial network model with a corresponding realistic temporal model custom-built for that specific spatial network (in order to be able to generate a spatiotemporal network model from a solely spatial network model). We validate the accuracy of our proposed modeling framework via experiments. We also used the proposed framework to generate the temporal model of the Los Angeles County freeway network and publish it for public use.

## 1. INTRODUCTION

The latest developments in online map services (e.g., Google Maps) and their widespread usage in hand-held devices and car-navigation systems have led to the recent prevalence of the location-based services. Many of the location-based services rely on efficient computation of the shortest path between a source and a destination in road networks. While the majority of the previous studies (e.g., [16, 10, 12, 3]) simplistically assume the travel-time of each segment of the network is constant, in reality the actual travel-time of a segment heavily depends on the traffic flow on the segment; hence, varies as a function of time. Recently, an increasing number of studies [8, 4, 5] consider time-dependent shortest path computation in road networks. However, most of these studies resort to using simplistic models and/or synthetic datasets to represent the temporal aspect of the road networks, mainly because collecting and working with real temporal data from road networks is costly and difficult, and the available temporal datasets are often proprietary and cannot be released for public use. Obviously, inaccurate temporal representation of road networks can seriously affect the validity of the design and evaluation of any proposed path planning technique for such networks; hence, the need for realistic models for traffic flows in spatiotemporal networks.

In this paper, we propose a framework for realistic and accurate modeling of traffic flows on road networks. The benefit of the proposed framework is twofold. First, anyone (e.g., governmental agencies) in possession of a real traffic data collected from a road network can use the proposed framework to derive and generate a realistic temporal model for the corresponding network, to be shared for public use (e.g., for researchers and policy planners) without infringing the copyright laws and jeopardizing the privacy of the dataset. As an example, we have used the proposed framework to generate and publish a realistic model for traffic flows in all freeways of the Los Angeles County based on the real (and proprietary) data provided to us by the county (see Section 4.1 for more details about this dataset)[1]. Second, as we describe in Section 4 (since the traffic in Los Angeles County is arguably typical and generic) one can use the proposed framework to generate realistic traffic flows specific to and customized for any given road network; hence, transferring the road network model to its corresponding spatiotemporal network model. Towards this end, we use a semi-supervised hierarchial clustering approach (based on the spatial characteristics of the network) to generate the spatiotemporal model of the network. To the best of our knowledge, our work is the first attempt in generating realistic temporal models for road networks.

The remainder of this paper is organized as follows. In Section 2 we review the related work. In Section 3 we provide the preliminary definitions, and subsequently in Section 4 we establish the theoretical foundation of our proposed traffic flow modeling framework and discuss the three-phase modeling process of this framework. In Section 5, we present the results of our experiments to verify and validate the accuracy of this framework. Finally, in Section 6 we conclude and discuss our future work.

## 2. RELATED WORK

In [2], Brinkhoff introduces a system called Network-based Generator of Moving Objects that models and simulates the behavior of moving objects (e.g., vehicles) on road networks. This system has been extensively used to benchmark k-nearest neighbor and location based search algorithms in road networks. While the focus of this system is the moving objects and their mobility in road networks, we primarily study to model the traffic flow on the network segments. In addition, this work relies on some simplistic assumptions about the network parameters such as minimum and maxi-

[1] http://infolab.usc.edu/projects/transdec/model.html


*IWCTS* '09 November 3, 2009, Seattle, WA, USA.

mum speed assignment for the network segments.

The freeway Performance Evaluation Monitoring System (PeMS) [13] developed by UC Berkeley collects and stores data from loop detectors operated by Caltrans. The main goal of PeMS is to convert the freeway sensor data into graphs and tables that show performance measures and traffic patterns on freeways in the State of California. The scope of PeMS is limited to collection and analysis of the historical freeway sensor data. However, our goal is to model the traffic flow for any given road network (even without sensor data) as described in Section 4.

Most of the traffic simulators developed in the recent decade use microscopic simulation models (aka, agent-based models) [14, 6] to simulate the traffic flow in road networks. The microscopic simulation models focus on the behavior of the system entities (e.g., vehicles and drivers) as well as their interactions with the system parameters (e.g., traffic lights). For instance, for each vehicle in the stream, a lane-change is described as a detailed chain of drivers' decisions. These simulation models, however, ignore the global descriptions of the traffic flows such as flow-rate, density and velocity and often are restricted to synthetic or simplified data.

There also exist several machine learning techniques developed for the purpose of traffic modeling. In [7], Kamarianakis et al. proposed a space-time autoregressive integrated moving average model to estimate the traffic flows on road networks. In [9], Lint et al. introduced a neural network based technique to model the traffic flow on freeways. However, all of these approaches are univariate and ignore most important factors such as road network geometry and spatiotemporal characteristics of the traffic flow.

# 3. DEFINITIONS

In this section, we formally define a road network with traffic flow as a spatiotemporal network. We assume a spatial network (e.g. the Los Angeles road network) containing a set of nodes and segments. We model the spatial network as a time-dependent weighted graph (i.e., spatiotemporal network) where the weights are time-varying travel-times (i.e., traffic flow) between the nodes. Below, we formally define our terminology

DEFINITION 1. *Spatiotemporal Network*
*A Spatiotemporal Network is defined as a graph $G_T(V, E, W)$ where $V = \{v_i\}$ is a set of nodes representing the intersections and terminal points, and $E$ ($E \subseteq V \times V$) is a set of edges representing the network segments each connecting two nodes. Each edge $e$ is represented by $e(v_i, v_j)$ where $v_i$ and $v_j$ are starting and ending nodes, respectively, and $v_i \neq v_j$. For every edge $e(v_i, v_j) \in E$, there is an edge travel-time function $w_{i,j}(t) \in W$, where $t$ is the time variable in time domain $T$. An edge travel-time function $w_{i,j}(t)$ specifies how much time it takes to travel from $v_i$ to $v_j$ starting at time $t$.*

Figure 1 illustrates a spatiotemporal network modeled as $G_T(V, E, W)$. While Figure 1(a) shows the network structure with five nodes and five edges, Figures 1(b), 1(c), 1(d), 1(e), 1(f) illustrate the time-dependent edge costs (i.e., travel-times) for the edges of the network.

# 4. METHODOLOGY

Our modeling framework is based on the real-world traffic data collected from the freeways in Los Angeles County (LA). The proposed framework offers solutions to the following two cases. In the first case, given the historical temporal data (time-series of traffic flow possibly collected from various sensor locations) of a road network, our framework creates the spatiotemporal model of that

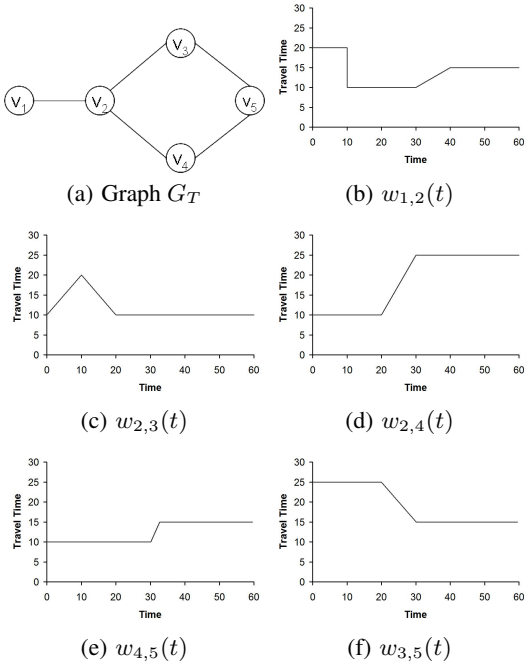


(a) Graph $G_T$ (b) $w_{1,2}(t)$

(c) $w_{2,3}(t)$ (d) $w_{2,4}(t)$

(e) $w_{4,5}(t)$ (f) $w_{3,5}(t)$

**Figure 1: A Spatiotemporal network $G_T(V, E, W)$**

network using the temporal data only. We refer to this case as Modeling with Temporal Data ($MTD$). However, the temporal data may not be available for most of the road networks as acquiring such data is a complex and sometimes prohibitively expensive task. In this (second) case, our framework generates a spatiotemporal network model from the *spatial characteristics* and the topology of the road network. We refer to the second case as Modeling with Spatial Characteristics ($MSC$).

Our approach involves the following three steps. In the first step, we compute the time-dependent travel-times on each network segment using historical time-series sensor data (*traffic flow generation*). In the second step, we attach semantic information to the network by labeling the regions of the network based on its spatial characteristics (*spatial characterization*). Finally, in the third step, we employ a semi-supervised clustering algorithm to group the traffic flows of similar kind into respective spatial characteristics by using the data obtained in the first and second steps (*hierarchical semantic traffic flow clustering*). The main idea here is to find the most representative traffic flows in and between the network regions based on their spatial characteristics. As we describe in Section 4.3.2, the traffic flows found in the final step can be used to model the traffic of any given road network without temporal data. Specifically, one can transfer any road network model to its corresponding spatiotemporal network model by using the similar spatial characteristics introduced in our model. While the techniques developed in the first step can result in $MTD$, we employ the second and third step to achieve $MSC$. Below, we explain each of these steps in turn.

## 4.1 Traffic Flow Generation

In the past one year, through a system called RIITS [15], we have been continuously collecting and archiving the sensor (i.e., loop detector) data from a collection of approximately 1500 sensors located on the freeways of LA County. The urban area of Los Angeles County has an area of 4752 square miles (12,308 $km^2$) and population of approximately nine million people. Figure 2 shows

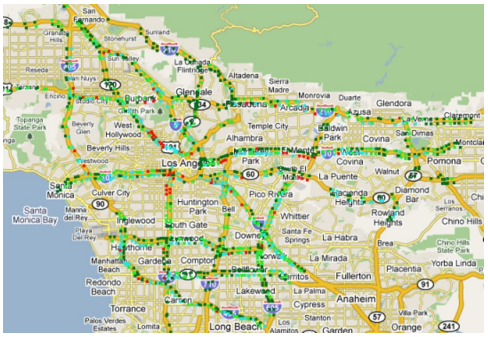


**Figure 2: Traffic sensor layout in LA County**

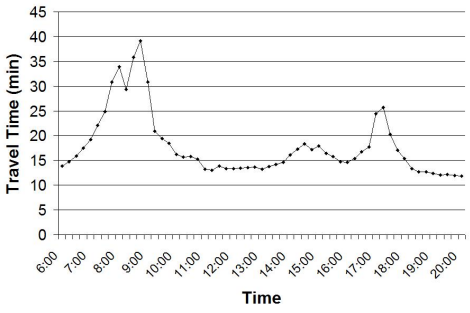


**Figure 3: Real travel-time during a weekday on a segment of I-405 in LA County**

the spatial span (covering 1183 miles) of the traffic sensors on a map. The sampling rate of the sensor data is 1 reading/sensor/min. We average the readings over three consecutive time intervals in order to ease the implementation and smooth out the noise. Therefore, each sensor provides 480 distinct measurements per day. We only consider the readings during the weekdays. The storage space required for this streamed dataset is approximately 350 MB/day without indexing overheads. Currently, our data warehouse consists of data from the period of October 2008 to June 2009.

The main traffic parameters collected from the loop detectors are *occupancy* and *volume*. The loop detectors turn on and off as cars pass over them. The number of *'on'* readings within a time interval (e.g., 60 seconds) determines the occupancy measure. Occupancy is defined as the percentage of time a point on network segment is occupied by vehicles. The other parameter, volume, is defined as the number of vehicles flowing past a point during a time interval. We derive a third parameter, speed, from the occupancy and volume readings using the formula introduced in [1] $Speed = \frac{C*V}{O}$ where $C$ is a constant proportional to the average length of a car, $V$ is volume, and $O$ is occupancy.

In order to determine the time-dependent travel-time on each network segment, we employ a two step process. First, using the spatial query operators, we map the coordinates of the individual sensors to network segments. Then, for each segment, we aggregate the desired traffic measure in both time and space dimensions by considering the distances between the sensors. For instance, for a given time instance, we compute the travel-time of a segment by the following formula $Travel\_Time = \sum_{i=1}^{n} \frac{D(s_i, s_{i+1})}{S_i}$ where $S_i$, $D(s_i, s_{i+1})$ and $n$ represents the speed measured on sensor $i$ at time $t$, the distance between two consecutive sensors, and the number of sensors on the segment, respectively. Figure 3 shows the graph of travel-time on a segment of I-405 freeway in LA between 6:00 AM and 8:00 PM on a weekday.

## 4.2 Spatial Characterization

In this section, we describe how we characterize the road network using geographical and topological characteristics of the network. Studying the real-world traffic data, we observe the following three main spatial and temporal characteristics of the traffic flow which motivated us to pursue the approach discussed in Section 4.3. First, the traffic flow on network segments demonstrates a strong *periodicity* at various spatial and temporal scales (daily, weekly, monthly, and quarterly). For example, the traffic flow on particular segment may exhibit a huge peak on each day at around 8:00 AM, a smaller one at around 4:00 PM, and an absolute minimum at around 2:00 AM during the weekdays in fall season. Second, the traffic flow is highly affected by the *spatial characteristics* of the network. That is, the traffic flow follows different patterns near major residential areas, city centers (aka, downtown), attraction areas (e.g., shopping centers, sports stadiums), and the regions in between. For instance, while a segment connecting a residential area to downtown is congested during morning hours, the opposite segment connecting downtown to a residential area is usually congested in the afternoon. Third, the traffic flows are also affected by the topology (i.e., another spatial characteristic) of the network. For example, a dense network topology which contains numerous nodes (hence many alternative routes) is usually congested in the hubs (i.e., intersection of the nodes) depending on the time of the day but has steady traffic flow in the rest of the region.

As we discussed, the main idea behind incorporating the spatial characteristics of the network to our model comes from the observation that the traffic flow in certain parts of the network can be affected by the geographical and topological characteristics. Although, there are various other characteristics (e.g., population and demographics) that are also good candidates to characterize a road network, we select two major characteristics for the purpose of this study namely, geographical region and density. We plan to include more spatial characteristics into our model in the future. For our study, we developed a graphical user interface (i.e., a map mashup) that enables users to label the geographical regions (i.e., residential, downtown, and attraction) of the road network. To capture the density information, the map interface allows users to partition the road network into regular grid cells (e.g., 5x5 km) and label the subnetworks (overlapping the grid cells) as dense or sparse based on the distribution of the number of nodes in each grid cell. Note that the map interface allows users to control the grid cell size. Clearly, these characteristics do not consider all possible aspects of the traffic flow and their specific definitions may vary. Our main focus is to establish a framework that considers the spatial characteristics of the road network for generating a spatiotemporal network model. We emphasize that our framework allows users to select their preferred spatial characteristics among the pre-defined ones. For example, one can only select regional information (ignoring density) to generate the spatiotemporal model of a particular network. In the following section, we explain how we incorporate the spatial characteristics of a network in to our proposed semi-supervised clustering algorithm.

## 4.3 Hierarchical Semantic Traffic Flow Clustering

The goal of this step is to cluster the time-series data constructed in Section 4.1 by enforcing the spatial characteristics mentioned in Section 4.2. Such clustering enables us to find the most representative traffic flows for the corresponding network regions. Towards this end, we propose Hierarchical Semantic Traffic Flow Clustering ($HSTFC$) method that is based on the semi-supervised clustering

algorithm introduced in [17]. Although the unsupervised clusters can identify the natural groups, it is extremely difficult to construct the mapping between the representation of the groups and their semantic meanings. Semi-supervised clustering addresses this issue by relating domain knowledge (in the form of labels and constraints) in to clusters. In other words, semi-supervised clustering not only creates natural groups with similar features but also provides semantic meanings to the cluster results. Therefore, in the context of our problem, semi-supervised clustering technique enables us to associate spatial characteristics of the network with their traffic flows. In the following sections, we first explain pairwise constraint clustering (a semi-supervised clustering method) and discuss how it fits in to our problem. Second, we present our proposed hierarchical clustering structure.

### 4.3.1 Pairwise Constraint Clustering Method

Pairwise constraint clustering ($PCC$) [17] is a classic technique to employ semi-supervised clustering. PCC, during the cluster computation, incorporates the domain knowledge (of the data instances) in the form of pairwise *cannot-link* and *must-link* constraints, and make the cluster results maximally satisfy the constraints. While *must-link* constraint specifies that two instances should be assigned into the same cluster, *cannot-link* constraint specifies that two instances should be assigned into different clusters. Let us now explain how this technique is adopted to our problem. As we discussed, in typical transportation networks, segments demonstrate different traffic patterns based on their geographical areas. For example, the traffic pattern of freeways near downtown may be entirely different than that of a suburban area. On the other hand, the segments which are spatially close to each other (e.g., two freeway segments near Hollywood) may generate similar traffic patterns. Hence, we can capture the knowledge in the latter case in the form of *must-link* constraint and the former case in the form of *cannot-link*. The formulation of pairwise constraint clustering is given below.

Let $M$ be the set of must-link pairs such that $(x_i, x_j) \in M$ implies $x_i$ and $x_j$ should be assigned to the same cluster, and $C$ be the set of cannot-link pairs such that $(x_i, x_j) \in C$ implies $x_i$ and $x_j$ should be assigned to different clusters. Let $W_m = w_{ij}$ and $W_c = \overline{w}_{ij}$ be the two sets that give the weight to the constraints in $M$ and $C$, respectively. Let $l_i$ be the assigned cluster number of instance $x_i$, and $\mu_{l_i}$ be the centroid of the cluster $l_i$. The cost of violating these pairwise constraints is typically the sum of violating pair(s) times their penalty weight. Specifically, the cost of violating a must-link constraint is given by $w_{ij} * f(l_i \neq l_j)$, where $f$ is the indicator function, with $f(true)$ = 1 and $f(false)$ = 0. Similarly, we could get the cost of violating the cannot-link constraint as $\overline{w}_{ij} * f(l_i = l_j)$. Using this model, the problem of PCC is formulated as the minimization problem on the following objective function:

$$\frac{1}{2} \sum_{x_i \in D} \|x_i - \mu_{l_i}\|^2 + \sum_{(x_i, x_j) \in M} w_{ij} * f(l_i \neq l_j) + \sum_{(x_i, x_j) \in C} \overline{w_{ij}} * f(l_i = l_j)$$

Algorithm 1 presents our pairwise constraint (k-means) clustering algorithm. The algorithm takes the dataset of the traffic flow ($D$), a set of must-link constraints ($M$), and a set of cannot-link constraints ($C$). Note that $M$ and $C$ are derived from the spatial characterization step. First, we call the function *POPULATE-CONSTRAINTS* to generate transitive closure over pair-wise constraints denoted as $M', C'$. Next, we initialize the cluster center by choosing $k$ points from the cannot-link constraints pairs in $C'$ as long as they do not have must-link constraints in $M'$. If we cannot find such $k$ points, we terminate the algorithm to enrich the input constraint set from the dataset, and restart. Finally, the algorithm returns the centroids of clusters that satisfy all the specified constraints. It is important to note that with Algorithm 1, we utilize the pairwise constraints for initializing the cluster centroid. For example, if two instances have cannot-link constraint, they should have distinct spatial category information. This enables us to guide the clustering process that generates two clusters maintaining distinct spatial characterizations. We assume that the cluster number (i.e., $k$) is equal to the number of pre-defined spatial characteristics.

**Algorithm 1** Pairwise Constraint K-means Clustering Algorithm

**Input**: Traffic flow D, must-link constraints $M \subseteq D \times D$, cannot-link constraints $C \subseteq D \times D$, Cluster Number k

**Output**: The cluster index of each variable $l_1, ...l_n$

1: Call POPULATE-CONSTRAINTS($M, C$);
2: Initialize the cluster center $\mu_1, ...\mu_k$
3: For each point $x_i$ in $D$, assign it to the closest cluster $l_j$ such that VIOLATE-CONSTRAINTS($di, l_j, M, C$) is false.
4: For each cluster $C_i$, update its center by averaging all of the points $d_j$ that have been assigned to it.
5: Iterate between (3) and (4) until convergence.
6: Return $l_1, ...l_n$.

POPULATE-CONSTRAINTS(must-link constraints set M, cannot-link constraints set C)

1: For each a: if both $(a, b), (a, c) \in M$, $M = (b, c) \cup M$
2: For each a: if $(a, b) \in M$, and $(a, c) \in C$, $C = (b, c) \cup C$
3: Return $M$, $C$ and denoted as $M'$, $C'$

VIOLATE-CONSTRAINTS(data point x, cluster L, must-link constraints M, cannot-link constraints C)

1: For each $(x, y) \in M$: If $y \notin L$, return true.
2: For each $(x, y) \in C$: If $y \in L$, return true.
3: Otherwise, return false.

### 4.3.2 Hierarchical Pairwise Constraint Clustering

So far we have explained the pairwise constraint clustering, but $PCC$ itself is not sufficient to solve our problem. This is because, some network segments may lead to multiple (and possibly contradictory) pairwise constraints depending on their spatial characterization. For example, let us consider both region and density information as two types of spatial characteristics that guide the pairwise constraint clustering. During the must-link and cannot-link constraint construction, two instances which have the same density value may lead to a must-link constraint. Meanwhile, a cannot-link constraint may also be assigned to these two instances due to their difference in the region values. In this case, since the two instances have both must-link and cannot-link constraints simultaneously, $PCC$ technique will suffer. To avoid this problem, we propose a hierarchical pairwise constraint clustering method that guides the clusters in multiple levels by considering a single type of characteristics at each level. It is important to note that our hierarchical structure makes it very easy to add new characteristics (e.g., segment length) to the system. Currently, we only have two hierarchies namely, region and density.

Fig.4 depicts an example of our hierarchical clustering method for two spatial characteristics namely, region and density. As illustrated, at the first level, the region information is used to compute the initial clusters. At the second level, based on the results from the first level, the density information is used to guide the semi-supervised clustering. Finally, the output are the traffic flows (i.e., centroid of clusters) corresponding to each spatial characteristics.

Let us now explain how this step is useful to achieve $MSC$ case

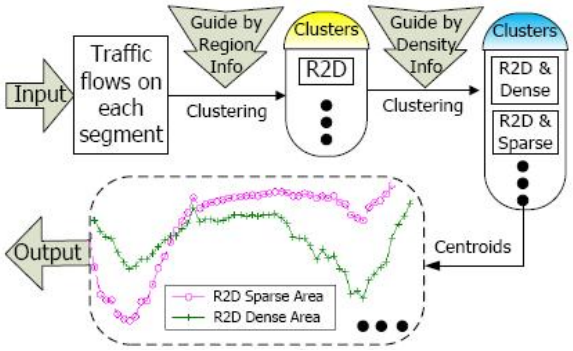


**Figure 4: Hierarchical semantic clustering flowchart.**

discussed in Section 4. As we explained, after clustering the traffic flows (for LA county dataset) based on the pre-defined spatial characteristics, we obtain a representative traffic flow (i.e., cluster centroid) corresponding to each spatial characteristics. Assuming that the traffic pattern in LA county is typical and generic, we use the proposed framework to generate the traffic flow for any given road network that has no temporal data but has similar spatial characteristics. Specifically, given a road network and its spatial characterization, we first group the network segments based on their spatial characteristics and then assign each group the corresponding cluster centroid obtained from LA county dataset.

# 5. PERFORMANCE EVALUATION

## 5.1 Experimental Setup

We conducted several experiments with different road networks and parameters to evaluate the performance of our algorithm. As we mentioned in Section 4.1, we used the real-world Los Angeles freeway traffic sensor data to construct our model. Since the traffic flow on freeways is much simpler than that of the local road network (i.e., no traffic light, no pedestrian), it requires less characterization. Therefore, to simplify our experiments, we only evaluated our model on freeway data. The sensor dataset is collected from 1592 sensors on the freeways during the period from October 2008 to June 2009. In order to represent the traffic flow on each segment, we computed the average travel time (from the historical sensor data) from 6:00 AM to 9:00 PM with 15 minute time intervals. As our road network dataset, we used Los Angeles ($LA$) and San Joaquin County ($SJ$) freeway network data. We obtained these datasets from NAVTEQ [11]. Using NAVTEQ dataset, we constructed the graph G(V,E) representation of LA and SJ freeway networks. Each network segment is represented in the vector data format and described by more than 20 attributes such as direction, speed limit, zip code, location, density, geographical location (e.g., residential), etc. Based on the location and direction information, we labeled the freeway segments into eight spatial categories namely, *RR*, *R*, *D*, *A*, *R2D*, *D2R*, *R2A*, *A2R*. The descriptions of these labels are presented in Table 1. Moreover, in addition to region labels, we defined another label capturing the density information of the network segments. In order to assign density label to the network segments, we partitioned both LA and SJ freeway networks into 5 $\times$ 5 km regular grid cells. Based on the average number of nodes($\alpha$) in each grid cell (assuming uniform distribution of the nodes), we labeled the segments as *Dense Area* (i.e., area that has more nodes than $\alpha$) or *Sparse Area*. We conducted our experiments on a workstation with 2.7 GHz Pentium Core Duo processor and 12GB RAM memory. Due to the space constraints, we only present the experimental evaluations from LA dataset.

**Table 1: Spatial Label Description**

| Label | Spatial Information for Freeway Segments |
|---|---|
| R | Residential Area |
| RR | Remote Area, area far from downtown and res. |
| D | Downtown Area |
| A | Attraction Area |
| R2D | From Residential Area to Downtown Area |
| D2R | From Downtown Area to Residential Area |
| R2A | From Residential Area to Attraction Area |
| A2R | From Attraction Area to Residential Area |

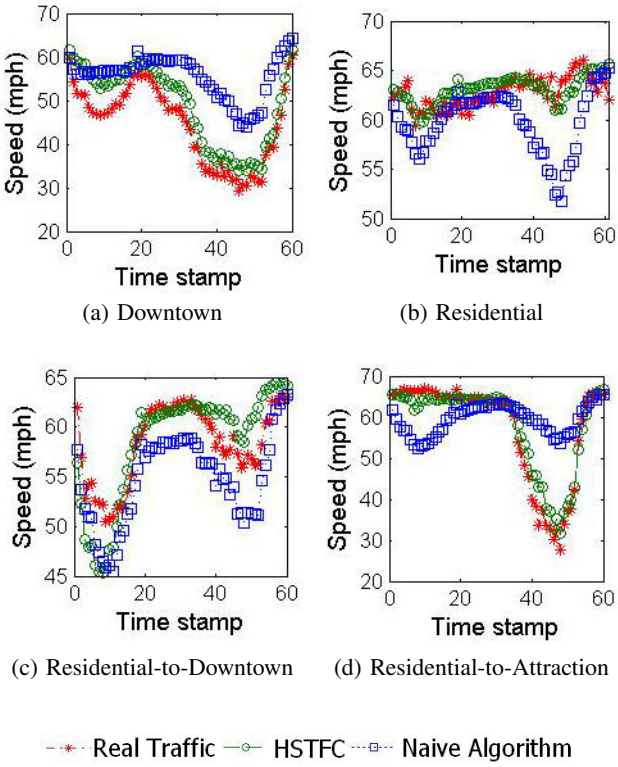


(a) Downtown (b) Residential

(c) Residential-to-Downtown (d) Residential-to-Attraction

**Figure 5: Traffic flow comparison**

## 5.2 Performance Study

For performance evaluation, we compared our algorithm with a naive approach that is based on decision tree. To implement decision tree, we used eight spatial categories (represented in Table 1) and density information (i.e., dense or sparse) as the nodes of the decision tree. The leaves of the decision tree contained the traffic flow information of the segments in the same category. Since each leaf can contain more than one traffic flow, we took the average value of the traffic flows to represent the corresponding leaf with one traffic flow. In our experiments, we measured the traffic flow similarity, general error rate and confidence interval.

### *5.2.1 Traffic Flow Similarity Comparison*

In this set of experiments, we compare the traffic flow obtained from the two algorithms with actual (observed) traffic flow on the segments. We randomly choose one instance in four categories: $D$, $R$, $R2D$, $R2A$. Figure 5 shows the traffic flow with respect to these four categories. The graphs cover the period from 6:00 AM

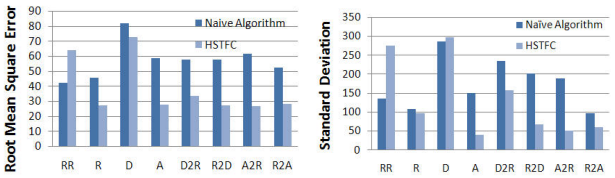


(a) Mean (b) Variation

**Figure 6: General error rate comparison**

(represented as 0 in the figures) to 9:00 PM with 15 minutes time intervals. As illustrated, the traffic flow generated by our HSTFC algorithm is more consistent with actual traffic flows. This is because, in real-world, some traffic patterns do not follow the major traffic flow trend in the same category due to some special events (e.g., accidents, lane closure). However, the naive decision tree approach considers that each instance contributes equally towards the construction of the category presentation. This assumption causes the results deviate from the major pattern trend hence leading to imprecise traffic flow representation. On the other hand, HSTFC considers both the spatial correlations and the traffic flow features; therefore, the centroid is calculated only based on the major trend of each category without possible noisy instances.

### 5.2.2 *General Error Rate Comparison*

In the second set of experiments, we compare the overall performance of two algorithms based on average root mean square error (MSE) and standard deviation(STD). These two measures enable us to quantify the amount by which the estimated centroids differ from the real instances. MSE and STD are calculated based on the distances between an individual instance and its corresponding centroid. The lower the value of these measures, the more precise the corresponding algorithm. Figure 6 depicts the performance of the two algorithms with respect to eight spatial categories. In general, the results show that the naive approach is less accurate than our algorithm with respect to both MSE and STD measures except for the RR category. The reason is that for RR, we require more types of characterizations to capture its traffic flow.

### 5.2.3 *Confidence Interval Evaluation*

In the final set of experiments, we use confidence intervals (CI) to indicate the reliability of our estimates. In particular, we evaluate the intensity of the featured clusters generated by the algorithms using CI. We consider the level of confidence interval is 90%, and use the mean of all distances between the instances and their cluster centroids as the observed mean value. Therefore, the lower the mean value, the denser the cluster. Figure 7 depicts the Euclidean distance between the instances and the cluster centroids (Y-axis) for eight spatial categories (X-axis). As illustrated, the naive algorithm has more sparse population of instances in each category.

## 6. CONCLUSION AND FUTURE WORK

In this paper, we introduced a framework for realistic and accurate modeling of traffic flows in road networks. We explained the design and implementation of our framework based on a real-word traffic sensor dataset. We intend to extend this work in two directions. First, we plan to extend the set of spatial characteristics supported by our framework to a complete minimum set that allows for modeling all typical road networks. Second, we plan to incorporate temporal characteristics (e.g., congestion intervals) of the road networks into our framework.

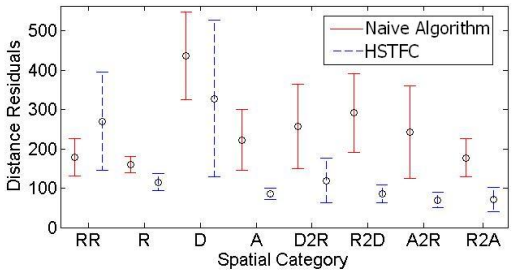


**Figure 7: Confidence interval evaluation**

## 7. ACKNOWLEDGMENTS

This research has been funded in part by NSF grants IIS-0238560 (PECASE), IIS-0534761, and CNS-0831505 (CyberTrust),the NSF Center for Embedded Networked Sensing (CCR-0120778) and in part from the METRANS Transportation Center, under grants from USDOT and Caltrans. Any opinions, findings, and conclusions expressed in this material are those of the author(s) and do not necessarily reflect the views of the National Science Foundation.

## 8. REFERENCES

[1] P. Athol. Interdependence of certain operational characteristics within a moving traffic stream. In *TRB*, 1967.

[2] T. Brinkhoff. A framework for generating network-based moving objects. In *Geoinformatica*, 2002.

[3] U. Demiryurek, F. B. Kashani, and C. Shahabi. Efficient continuous nearest neighbor query in spatial networks using euclidean restriction. In *SSTD*, 2009.

[4] B. Ding, J. X. Yu, and L. Qin. Finding time-dependent shortest paths over large graphs. In *EDBT*, 2008.

[5] B. George, S. Kim, and S. Shekhar. Spatio-temporal network databases and routing algorithms: A summary of results. In *SSTD*, 2007.

[6] S. P. Hoogendoorn and P. Bovy. State-of-the-art of vehicular traffic flow modelling. In *Journal of Systems and Control Engineering*, 2001.

[7] Y. Kamarianakis and P. Prastacos. Space-time modeling of traffic flow. 2007.

[8] E. Kanoulas, Y. Du, T. Xia, and D. Zhang. Finding fastest paths on a road network with speed patterns. In *ICDE*, 2006.

[9] H. v. Lint, S. P. Hoogendoorn, and H. J. v. Zuylen. State space neural networks for freeway travel time prediction. In *ICANN*, London, UK, 2002.

[10] K. Mouratidis, M. L. Yiu, D. Papadias, and N. Mamoulis. Continuous nearest neighbor monitoring in road networks. In *VLDB*, 2006.

[11] Navteq. http://www.navteq.com. Last visited June 17, 2009.

[12] D. Papadias, J. Zhang, N. Mamoulis, and Y. Tao. Query processing in spatial network databases. In *VLDB*, 2003.

[13] PeMS. https://pems.eecs.berkeley.edu/. Last visited May 15, 2009.

[14] M. Pursula. Simulation of traffic systems-an overview. In *Journal of GIS and Decision Analysis*, 1999.

[15] RIITS. http://www.riits.net/. Last visited December 25, 2008.

[16] H. Samet, J. Sankaranarayanan, and H. Alborzi. Scalable network distance browsing in spatial databases. In *SIGMOD*, 2008.

[17] K. Wagstaff, C. Cardie, S. Rogers, and S. Schroedl. K-means clustering with background knowledge. In *ICML*, 2001.